A finite element model illustrating geosynthetic reinforcement mechanisms for paved roadways

S.W. Perkins, M.Q. Edens & Y. Wang
Montana State University, Bozeman, Montana USA

R.J. Fragaszy
National Science Foundation, Arlington, Virginia, USA

Keywords: Interface aspects, Numerical modeling, Pavement systems, Reinforcement, roads

ABSTRACT: Previous experimental work has shown the ability of geosynthetics to provide reinforcement and improve the permanent surface deformation performance of paved roadways, and has demonstrated the mechanisms by which reinforcement occurs. As part of an ongoing study whose goal is the development of a general design methodology for reinforced paved roads, a finite element model has been developed to predict the behavior of reinforced roads subject to repeated vehicular loading. The model contains constitutive relationships for the various pavement layer materials, the geosynthetic reinforcement and the contact interaction between the base aggregate and the geosynthetic that are capable of showing the accumulation of permanent strain and displacement under repeated load. The model is used to analyze a conventional unreinforced pavement, a geosynthetic reinforced pavement and a "perfectly" reinforced pavement created by constraining the lateral motion of the common nodes between the base and the subgrade. Results demonstrate the ability of the model to qualitatively match the reinforcement mechanisms seen in large-scale pavement test sections, and indicate the model's ability to realistically describe reinforced pavement performance.

1 INTRODUCTION

The design of paved roadways using a geosynthetic contained in the base course aggregate layer for purposes of reinforcement has been inhibited by the lack of a general purpose design procedure that is capable of accounting for variables that are known or suspected to impact the performance of the roadway. These variables include the thickness and perhaps the mechanical properties of the asphalt concrete and base course aggregate layers, the strength and deformation properties of the subgrade soil, the magnitude of load and number of repetitions of the vehicular traffic, the mechanical properties of the geosynthetic, the placement position of the geosynthetic within the base course layer, and the interaction properties between the geosynthetic and the surrounding materials (Perkins, Ismeik 1997a; Berg et al. 2000). Existing design solutions typically have been empirically derived from a given set of experimental results and are therefore limited to the conditions for which the experiments were constructed (Perkins, Ismeik 1997b; Berg et al. 2000). Many of these design solutions are specific to a particular geosynthetic product, which further limits the designer's ability to compare products within the framework of a project specific economic analysis.

These limitations point to the need for an analytical tool that is general with respect to the input of a roadway's geometry and material properties. The finite element method presents a means of reaching this goal. Several studies exist that have used the finite element method for the analysis of reinforced pavements. Several early studies focused on the prediction of permanent deformation of unpaved roads subject to the application of one monotonically increasing load (Burd, Houlsby 1986; Burd, Brocklehurst 1990, 1992). Barksdale et al. (1989), Dondi (1994), Mirua et al. (1990) and Wathugala et al. (1996) describe the development of finite element models that were also pri-

marily intended for predicting deformation occurring over one cycle of load, but for paved roadways.

Three of the seven studies used soil-geosynthetic interface models capable of demonstrating permanent slip at the interface. One study used a material model for the geosynthetic that could predict permanent strain in this material (Wathugala et al. 1996). None of the studies used constitutive models for the base aggregate and subgrade soils that were capable of showing the accumulation of permanent strain with repeated vehicular loads. Perkins, Ismeik (1997b) have summarized the major features and results arising from these seven studies.

The material presented in this paper describes the development of a finite element model that can be used to predict the permanent deformation behavior of paved roadways subject to repeated loads and reinforced with geosynthetics. The model is currently being compared to experimental results and will be used to predict pavement response for a wide array of variables with the aim of developing a design solution based on this parametric study. This paper describes the general features of the model and presents predictions using generic material properties showing the ability of the model to qualitatively describe reinforcement mechanisms observed in large-scale test sections. Correctly describing these mechanisms is a critical first step for any model that will be subsequently used to predict reinforced pavement performance.

2 MODELING OBJECTIVE

Experience with large-scale reinforced pavement test sections has demonstrated that the benefits of geosynthetic reinforcement can be observed for a small number of load applications, however the eventual and often times more substantial benefits are not observed until a larger number of vehicular loads are applied. Given that the benefit of the reinforcement is defined by its ability to retard the development of permanent strain in the pavement layer materials, a model capable of predicting the development of permanent strain under repeated loading is necessary to fully predict the benefits of the reinforcement. For this reason, the finite element model described in this paper was developed to account for the long-term permanent deformation history of the pavement. This objective was accomplished by providing material models capable of showing this type of response and prescribing loading conditions that provide a repetition of load to the pavement surface.

3 ANTICIPATED REINFORCEMENT MECHANISMS

Experimental work with instrumented, geosynthetic-reinforced pavement test sections has demonstrated the mechanisms by which the geosynthetic provides reinforcement. Data illustrating these mechanisms have been presented by Perkins (1999) and consist of four mechanisms illustrated in Figure 1 and listed below:

1. Reduction of horizontal strain (ε_h), or lateral spreading, in the base course aggregate adjacent to the geosynthetic.
2. An increase in horizontal stress (σ_h) or confinement, and hence elastic modulus of the base aggregate.
3. A reduction of vertical stress (σ_v) in the top of the subgrade.
4. A reduction of shear stress (τ) in the top of the subgrade.

These mechanisms result in a reduction of permanent vertical strain in the base aggregate and subgrade soil layers and hence a reduction of permanent deformation of the pavement surface. A finite element model expected to offer reasonable predictions of reinforced pavement performance should be capable of showing these reinforcement mechanisms.

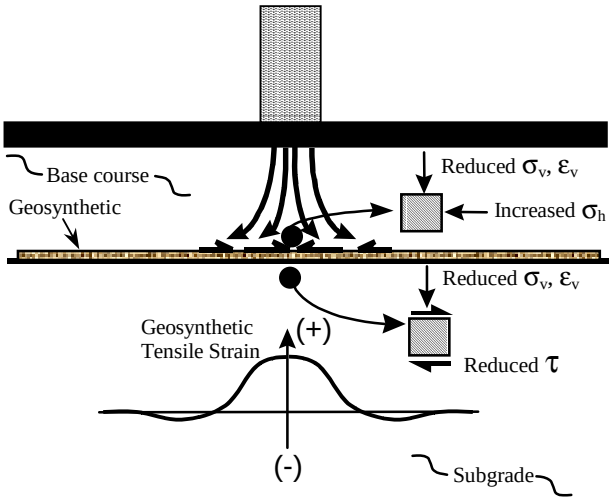

Figure 1. Reinforcement mechanisms.

4 MODEL GEOMETRY, LOADING AND MATERIALS

A finite element model has been assembled to match the conditions present in pavement test sections reported by Perkins (1999). These test sections were constructed in a large concrete box measuring 2 m by 2 m by 1.5 m in height. Traffic loading was simulated by applying a repeated load of 40 kN at a period of approximately 1.5 seconds to a rigid plate measuring 300 mm in diameter resting on a waffled rubber pad. Nominal thickness of the asphalt concrete (AC) and base aggregate layers in these test sections was 75 mm and 300 mm, respectively.

The finite element program ABAQUS (Hibbitt et al. 1999) was used to model this pavement test facility. Provided below is a description of the geometry, loading conditions and material models used.

4.1 *Model geometry*

A three-dimensional finite element model was developed to match the geometry of these pavement test sections and is shown in Figure 2. A 3-D model, as opposed to an axi-symmetric model, was used because of the corners of the box and the direction dependent properties of the geosynthetic. Symmetry of the box was recognized such that one-quarter of the box was modeled, with the vertical planes intersecting at right angles through the load plate centerline representing planes of symmetry. Eight-noded hexagonal solid elements were used for the asphalt concrete, base aggregate and subgrade soil layers, with approximately 230, 570 and 1600 elements being used for each layer, respectively. The nodes between the asphalt concrete and base aggregate layers were equivalenced and therefore connected. Four-noded quadrilateral membrane elements were used for the geosynthetic, with approximately 140 elements used. Membrane elements provide strength in the plane of the element but have no bending stiffness. These elements are well suited for representing thin, flexurally flexible layers such as geosynthetics.

Contact surfaces were specified between the top of the geosynthetic and the base aggregate soil. While a second set of contact surfaces could be specified between the bottom of the geosynthetic and the subgrade soil, this was not done in this analysis in an attempt to reduce computational time. In lieu of this second contact set definition, the nodes between the geosynthetic and the top layer of nodes of the subgrade were equivalenced and therefore connected. The use of contact surfaces allows for the definition of a model describing the shear stress – shear displacement interaction for the contact interface. Details of this are given in a following section on material models.

The boundary conditions for the box are seen with the aid of Figure 2. The two vertical planes of symmetry were specified by allowing motion in the vertical direction and in the horizontal direction within the plane but not in a horizontal direction perpendicular to the plane. With the exceptions noted below, the motion of nodes along the two vertical planes corresponding to the box walls were unconstrained in the z direction and constrained from horizontal motion perpendicular and parallel to the wall. The nodes along the edges of the asphalt concrete adjacent to the box walls were free in all directions to prevent any tensile stresses from developing as the asphalt might try to pull away from the box walls. Similarly, the nodes along the edge of the geosynthetic adjacent to the box walls were unconstrained in the x, y and z directions to allow inwards movement to prevent artificial membrane type stresses from developing. The bottom of the box was constrained from motion in the x, y and z directions.

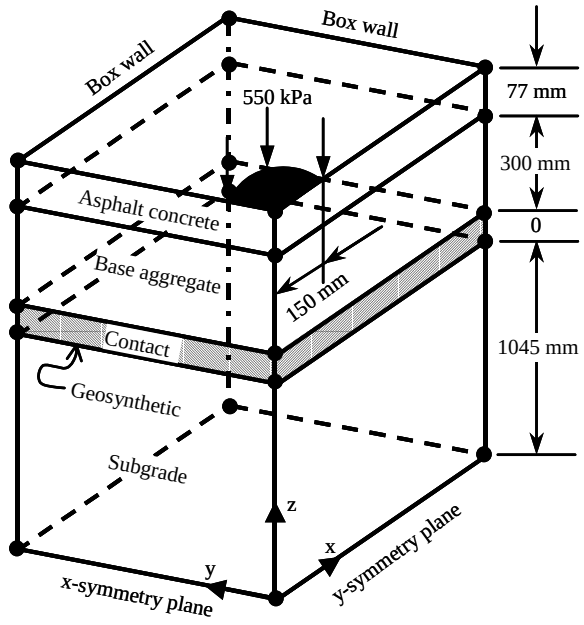

Figure 2. Model geometry, loading and boundary conditions.

4.2 *Model loading*

A uniform pressure of 550 kPa was applied as shown in Figure 2 along a ¼ circular area having a radius of 150 mm. Given the absence of any time dependent behavior in the material models used, the load was applied as a ramp load up to this pressure and then released to a value of 14 kPa. Plate pressure cycling between 550 kPa and 14 kPa was repeated for the desired number of load cycles. The minimum plate pressure during unloading was imposed to match similar conditions present in pavement test sections reported by Perkins (1999).

4.3 *Material models*

Material models for the AC, base aggregate, subgrade soils, geosynthetic and contact interface interaction were developed to allow for the accumulation of permanent strain and deformation under repeated load cycles. The model used for the asphalt concrete consisted of a linearly elastic – anisotropic perfectly plastic model. The plasticity component of the model was added to allow the AC layer to conform to the deformed shape of the underlying base aggregate and to prevent the application of upwards acting tensile stresses induced during unloading of the pavement. The anisotropic plasticity component was added to facilitate in-plane shear flow of the material while preventing excessive vertical compression of the layer. The model for the AC contains 9 parameters, namely 2 elastic constants (elastic modulus, E_{AC}, Poisson's ratio, ν_{AC}), an ultimate yield stress,

σ^{o}_{AC}, and six anisotropic plastic potentials. The ultimate yield stress is the strength of the material in uniaxial tension and compression.

Plastic potential is defined with respect to a yield stress ratio referenced to the value of σ^{o}_{AC}. The six values of anisotropic yield stress ratio are given by the expressions:

$$R_{11} = \frac{\overline{\sigma}_{11}}{\sigma^{o}_{AC}},\ R_{22} = \frac{\overline{\sigma}_{22}}{\sigma^{o}_{AC}},\ R_{33} = \frac{\overline{\sigma}_{33}}{\sigma^{o}_{AC}},$$
$$R_{12} = \frac{\sqrt{3}\overline{\sigma}_{12}}{\sigma^{o}_{AC}},\ R_{13} = \frac{\sqrt{3}\overline{\sigma}_{13}}{\sigma^{o}_{AC}},\ R_{23} = \frac{\sqrt{3}\overline{\sigma}_{23}}{\sigma^{o}_{AC}} \quad (1)$$

where each is the measured yield stress value when σ_{ij} is the only nonzero stress component applied and where the subscripts 1, 2 and 3 denote the x, y and z coordinate axes, respectively. Table 1 lists the values used for the analyses reported in this paper, where these values are comparable to those determined from indirect tension resilient modulus tests performed on AC cores from the test sections reported by Perkins (1999).

Table 1. Asphalt material properties.

Parameter	Value
E_{AC} (MPa)	3620
ν_{AC}	0.35
σ^{o}_{AC} (kPa)	880
$R_{11}= R_{22}= R_{33}$	1.0
$R_{12}= R_{13}= R_{23}$	0.5

The constitutive model used for the base aggregate and subgrade soil is based on the bounding surface plasticity model developed by Dafalias, Hermann (1986). A User Defined Material model (UMAT) was written and incorporated into ABAQUS. The model contains 11 parameters that can be calibrated from triaxial compression tests. Several of these parameters (λ, κ, M, ν) describe conventional critical state soil mechanics properties, while others are shape and hardening parameters associated with the bounding surfaces. The model includes a formulation for shear modulus, G, (Equation 2) that is dependent on the mean stress confinement or first invariant of stress, I, and where I_L is atmospheric pressure, ν is Poisson's ratio and e_{in} is the initial void ratio of the soil.

$$G = \frac{3(1-2\nu)(1+e_{in})}{6\kappa(1+\nu)}\left(\langle I - I_L \rangle + I_L\right) \quad (2)$$

The model parameters used in the analyses reported in this paper are listed in Table 2. Perkins et al. (2000) has described the model and its calibration in more detail. The parameters selected for the base aggregate represent a conventional, well-graded crushed river aggregate material compacted to a high degree of relative density. The parameters selected for the subgrade represent a weak material having a subgrade CBR of approximately 1.5.

An isotropic elastic-plastic model was used to model geosynthetic tensile behavior. The isotropic elastic constants used for the analyses reported in this paper consist of an elastic modulus and a Poisson's ratio having values of 1×10^{7} kPa and 0.1, respectively. An isotropic hardening rule was used for the plasticity component of the model and is specified by the curve of plastic strain versus axial stress given in Figure 3. More complex material models for the geosynthetic that account for direction-dependent elastic, plastic and time-dependent creep behavior have been developed for this problem (Perkins, 2000) but were not used for the results presented in this paper for sake of simplicity.

Table 2. Base and subgrade bounding surface model parameters.

Parameter		Value	
		Base	Subgrade
e_o	– Initial void ratio	0.5	1.5
λ	– Virgin compression slope	0.0075	0.24
κ	– Swell/recompression slope	0.001	0.12
M	– Slope of critical state line	1.7	0.65
ν	– Poisson's ratio	0.2	0.2
R	– Shape parameter	1.4	1.75
A	– Shape parameter	0.015	0.03
T	– Shape parameter	0.01	0.03
C	– Projection center parameter	0.0	0.0
s_p	– Elastic zone parameter	1.06	1.1
m	– Hardening parameter	0.02	0.02
h	– Hardening parameter	16	10
p_o	– Preconsolidation stress (kPa)	1250	315

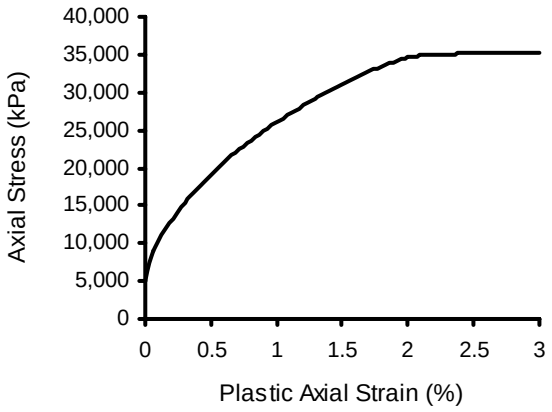

Figure 3. Geosynthetic isotropic hardening rule.

A Coulomb type frictional model was used to describe shear interaction between the contact surfaces consisting of the geosynthetic and the base aggregate. In the form used in this paper, the model contains two parameters as illustrated in Figure 4. These parameters are a friction coefficient (μ) defining the shear stress at which permanent slip begins to occur between the contact surfaces and an elastic slip displacement (E_{slip}) at which point permanent slip initiates. Both the gross shearing resistance and stiffness of the interface are a function of the normal stress on the interface. For the analyses reported in this paper, the friction coefficient was set to 1.428 (55°) while E_{slip}= 0.1 mm.

5 MODEL ILLUSTRATION OF REINFORCEMENT MECHANISMS

Three separate finite element models were created to examine the appropriateness of the model described above for exhibiting the reinforcement mechanisms presented earlier in this paper. The first model is one with geosynthetic reinforcement and consists of the components and parameters discussed above. The second model consists of an unreinforced pavement section with only asphalt concrete, base aggregate and subgrade having the same dimensions and properties as the reinforced section. For this case, the set of nodes at the bottom of the base and the corresponding set of nodes in the top of the subgrade were equivalenced and therefore connected. The third model is identical

to the second but with the x and y degrees of freedom for the set of common nodes between the base aggregate and subgrade layers completely constrained from motion in all horizontal (x, y) directions. This third case is an idealization of a case with an infinitely stiff reinforcement layer and with rigid or fixed contact between the interfaces and therefore represents "perfect" reinforcement. In subsequent discussion, these three cases are referred to as "reinforced", "unreinforced" and "fixed base", respectively. Each model was subject to ten cycles of load.

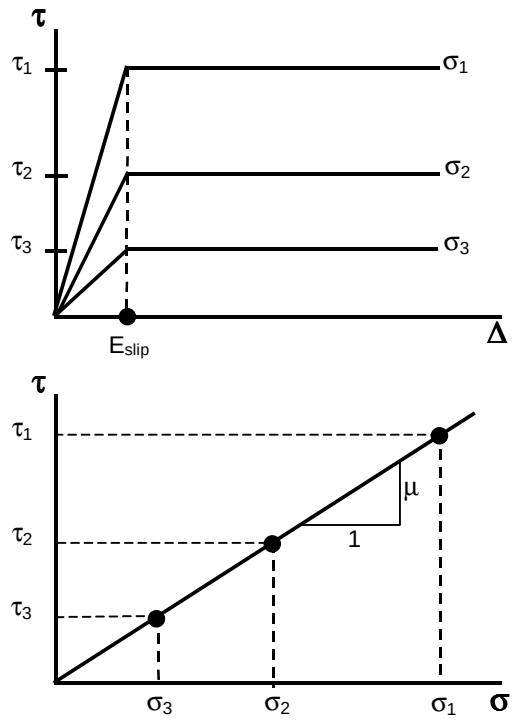

Figure 4. Contact surface interaction model.

Figure 5 illustrates the permanent horizontal strain in the x-direction along a line emerging from the load plate centerline and passing through the bottom of the base aggregate and along the symmetry plane after 1 cycle and 10 cycles of load have been applied, and where strains were interpolated from integration points. In this figure, negative strain corresponds to extension while positive strain corresponds to compression. Each set of data represents the permanent strain in the bottom of the base. As expected, the fixed base case shows no lateral strain as the nodes along the bottom of the base are fixed from motion in the x and y directions. The presence of reinforcement considerably limits the amount of lateral strain at this depth in the base and corresponds qualitatively to behavior seen in experimental test sections (Perkins 1999).

Figure 6 shows the permanent strain in the x-direction along a vertical line extending through the load plate center and plotted against depth throughout the pavement section after 10 cycles of load. The results show that the effect of restricting lateral motion of the base aggregate at the geosynthetic interface is seen by a reduction of lateral strain further up in the base aggregate and well into the subgrade soil with this effect being most pronounced for the fixed base case.

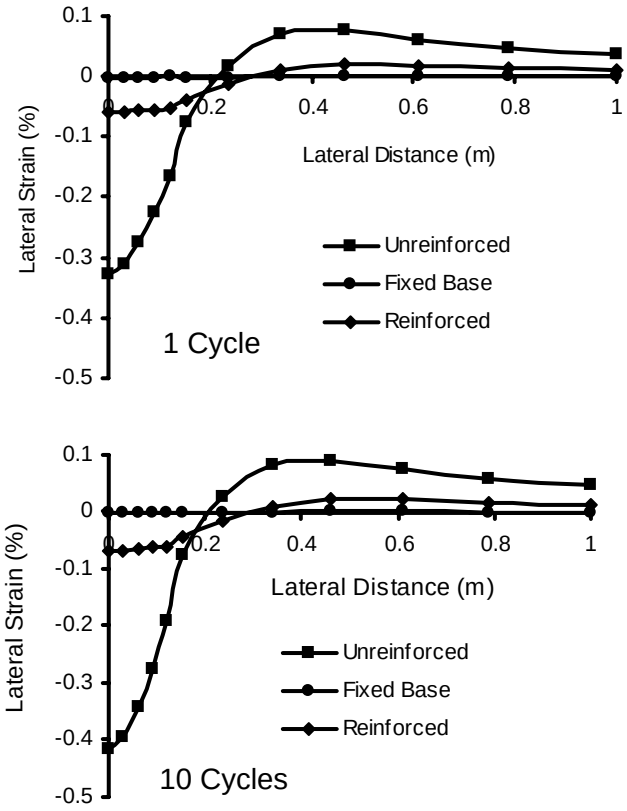

Figure 5. Lateral permanent strain in the bottom of the base versus lateral distance after 1 and 10 cycles of load.

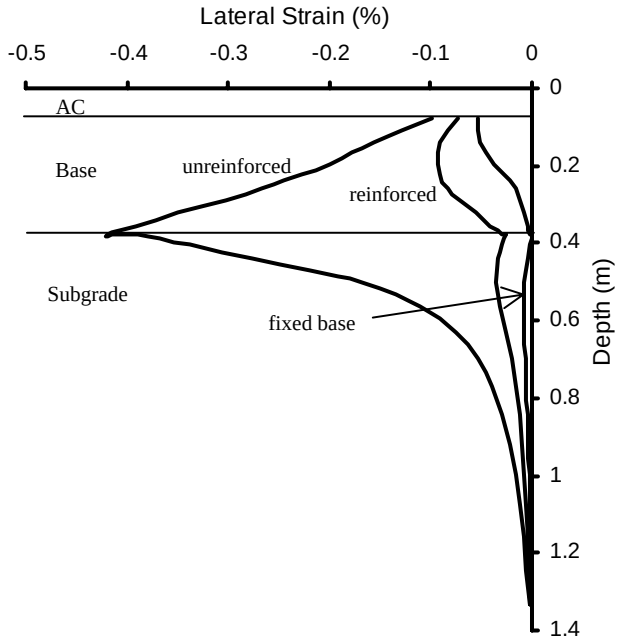

Figure 6. Lateral permanent strain along the load plate centerline versus depth after 10 cycles of load.

Figure 7 shows the mean stress, defined as the average of the three principal stresses, along the same horizontal line in the bottom of the base as used in Figure 5 and at the point where the peak pavement load was applied for the first load cycle. The results show that a restriction of lateral motion of the base aggregate results in an increase in mean stress, with this effect being most significant for the fixed base case. For these analyses, the increase in modulus of the base for the reinforced case is approximately 1.5 to 3 times that of the unreinforced case at this location. This effect begins to diminish for points higher in the base, as illustrated in Figure 8 for a position 70 mm above the bottom of the base.

Figure 9 shows the vertical stress along the top of the subgrade at peak load for the first load cycle. The effect of confinement and subsequent increase in modulus of the base is to reduce the peak vertical stress occurring under the load plate. Figure 10 shows data similar to Figure 5 showing that the lateral strain in the top of the subgrade is reduced by the use of reinforcement. The effect of these mechanisms is to reduce the permanent vertical strain beneath the load plate centerline and to reduce the amount of permanent surface deformation of the pavement, as illustrated in Figures 11 and 12.

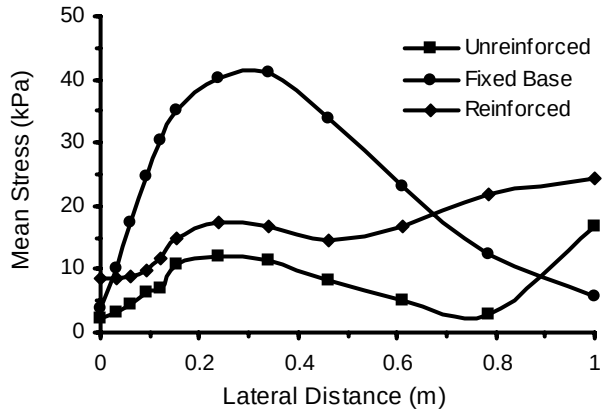

Figure 7. Mean stress at peak load along the bottom of the base.

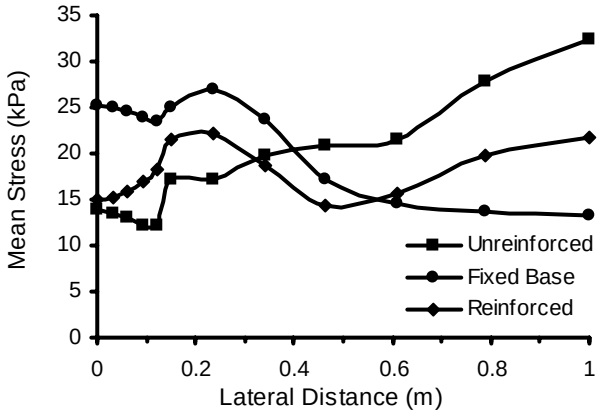

Figure 8. Mean stress at peak load along a line 70 mm above the bottom of the base.

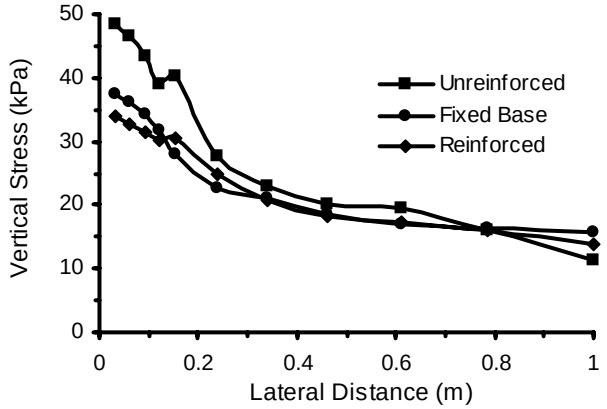

Figure 9. Vertical stress at peak load in the top of the subgrade.

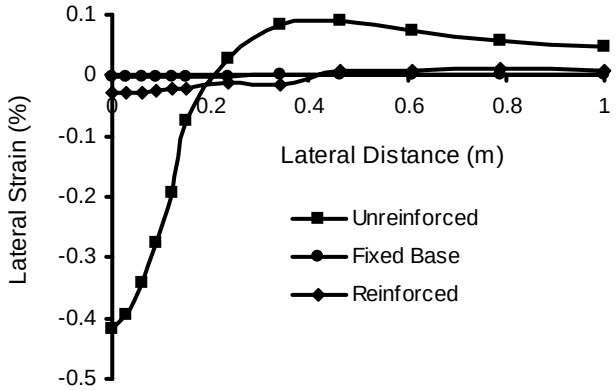

Figure 10. Lateral permanent strain in the top of the subgrade versus lateral distance after 10 cycles of load.

Figures 13 and 14 show the relative displacement between the interface contact surfaces and the interface shear stress versus lateral distance along the x-axis extending through the contact surface between the base aggregate and the geosynthetic. Results are shown for load cycles 1 and 10 for the point at which the load is a maximum and a minimum for the cycle. Figure 13 indicates that for this analysis, the value of E_{slip}= 0.1 mm is not exceeded but is being approached for 10 cycles of load application. This figure also shows the ability of relative displacement to accumulate with applied load cycle even though E_{slip} is not exceeded.

Figure 14 shows the level of shear stress that exists at the interface, which serves to retard lateral motion of the base aggregate. Comparison of Figures 13 and 14 shows that the increase in shear stress on the interface when the pavement load is fully applied is proportionally greater than the increase in relative displacement. Using Figure 4, it can be seen that in order for this to occur, the normal stress on the interface must be greater at peak load for cycle 10 as compared to cycle 1. An increase of normal stress and shearing resistance with applied load cycles is but one indication of the need for models that account for the effects of repeated load.

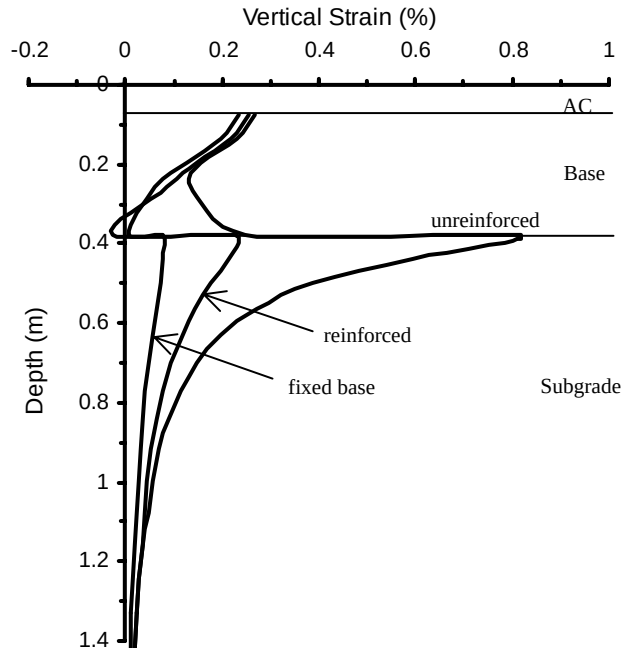

Figure 11. Vertical permanent strain along the load plate centerline versus depth after 10 cycles of load.

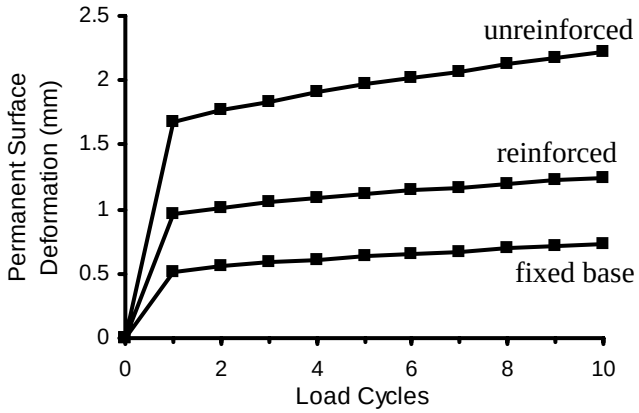

Figure 12. Permanent surface deformation versus applied load cycles.

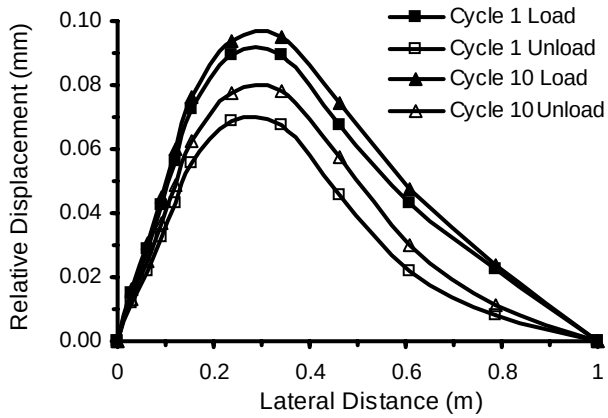

Figure 13. Relative displacement between the base aggregate and the geosynthetic interface.

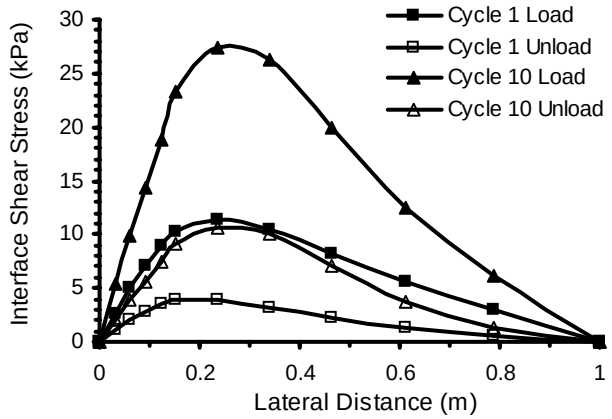

Figure 14. Interface shear stress between the base aggregate and the geosynthetic.

6 CONCLUSIONS

A finite element model has been formulated to contain material models that allow for the prediction of permanent strain and displacement of the pavement layer materials. Three models for cases of a conventional unreinforced pavement, a geosynthetic reinforced pavement and a “perfectly” reinforced pavement were created and analyzed for ten cycles of pavement load. The models used generic material properties for the various pavement layer, subgrade and geosynthetic materials. The “perfectly” reinforced pavement model was created by constraining the lateral motion of the nodes at the base aggregate – subgrade interface of the unreinforced pavement model. This case represents ideal reinforcement in the sense of artificially creating an infinitely stiff geosynthetic layer and rigid, or tied contact at the interface. The models show the ability of the reinforcement to improve the permanent surface deformation performance of the pavement. The model results obtained demonstrate reinforcement mechanisms that qualitatively agree with those demonstrated in earlier experimental work involving large-scale pavement test sections. The reinforced pavement case is seen to lie between the unreinforced case and the “perfectly” reinforced case.

ACKNOWLEDGMENTS

The authors gratefully acknowledge the financial support from a pool of eight state departments of transportation including Idaho, Kansas, Minnesota, Montana, New York, Texas, Wisconsin and Wyoming and the Western Transportation Institute at Montana State University.

REFERENCES

Barksdale, R.D., Brown, S.F., Chan, F. 1989. Potential Benefits of Geosynthetics in Flexible Pavement Systems. *National Cooperative Highway Research Program Report No. 315*, Transportation Research Board, National Research Council, Washington DC.

Berg R.R., Christopher, B.R., Perkins, S.W. 1999. *Geosynthetic Reinforcement of the Aggregate Base Course of Flexible Pavement Structures, GMA White Paper II*, Geosynthetic Materials Association, 130p.

Burd, H.J., Brocklehurst, C.J. 1990. Finite Element Studies of the Mechanics of Reinforced Unpaved Roads. *Proceedings of the 4th International Conference on Geotextiles, Geomembranes and Related Products*, The Hauge, Netherlands, pp. 217-221.

Burd, H.J., Brocklehurst, C.J. 1992. Parametric Studies of a Soil Reinforcement Problem Using Finite Element Analysis. *Proceedings of the Conference on Computer Methods and Advances in Geomechanics*, Balkema, pp. 1783-1788.

Burd, H.J., Houlsby, G.T. 1986. A Large Strain Finite Element Formulation for One Dimensional Membrane Elements. *Computers and Geotechnics*, Vol. 2, pp. 3-22.

Dafalias, Y.F., Hermann, L.R. 1986. Bounding Surface Plasticity. II: Application to Isotropic Cohesive Soils. *Journal of Engineering Mechanics*, ASCE, Vol. 112, No. 12, pp. 1263-1291.

Dondi, G. 1994. Three-Dimensional Finite Element Analysis of a Reinforced Paved Road. *Proceedings of the Fifth International Conference on Geotextiles, Geomembranes and Related Products*, Singapore, pp. 95-100.

Hibbitt, Karlson, Sorensen 1998. *ABAQUS Standard User's Manuals, Version 5.8*, Pawtucket, RI, USA.

Perkins, S.W. 1999. Mechanical Response of Geosynthetic-Reinforced Flexible Pavements. *Geosynthetics International*, Vol. 6, No. 5, pp. 347-382.

Perkins, S.W. 2000. Constitutive Modeling of Geosynthetics. *Geotextiles and Geomembranes*, Vol. 18, No. 5, pp. 273-292.

Perkins, S.W., Ismeik, M. 1997a. A Synthesis and Evaluation of Geosynthetic Reinforced Base Course Layers in Flexible Pavements: Part I. *Geosynthetics International*, Vol. 4, No. 6, pp. 549-604.

Perkins, S.W., Ismeik, M. 1997b. A Synthesis and Evaluation of Geosynthetic Reinforced Base Course Layers in Flexible Pavements: Part II. *Geosynthetics International*, Vol. 4, No. 6, pp. 605-621.

Perkins, S.W., Wang, Y., Edens, M.Q., Fragaszy, R.J. 2000. Prediction of Permanent Deformation in the Unbound Aggregate and Subgrade Soils of a Paved Roadway. *Unbound Aggregates in Road Construction*, Balkema, Rotterdam, Netherlands, pp. 377-384.

Wathugala, G.W., Huang, B., Pal, S. 1996. Numerical Simulation of Geosynthetic Reinforced Flexible Pavement. *Transportation Research Record 1534*, TRB, National Research Council, Washington, DC, USA, pp. 58-65.